



# Global Biogeochemical Cycles<sup>a</sup>

#### RESEARCH ARTICLE

10.1029/2023GB007995

#### **Key Points:**

- Satellite ocean color was used to describe variability in terrigenous dissolved organic carbon (tDOC) in the Amazon River plume
- tDOC degradation and/or flocculation over the shelf increase early in the year when river discharge also increases
- Interannual variability in tDOC content off the continental margin is related to variability in tDOC removal over the shelf

#### Correspondence to:

P. M. Medeiros, medeiros@uga.edu

#### Citation:

Martineac, R. P., Castelao, R. M., & Medeiros, P. M. (2024). Seasonal and interannual variability in the distribution and removal of terrigenous dissolved organic carbon in the Amazon River plume. *Global Biogeochemical Cycles*, *38*, e2023GB007995. https://doi.org/10.1029/2023GB007995

Received 7 OCT 2023 Accepted 31 MAY 2024

© 2024. The Authors.

This is an open access article under the terms of the Creative Commons

Attribution-NonCommercial-NoDerivs

License, which permits use and distribution in any medium, provided the original work is properly cited, the use is non-commercial and no modifications or adaptations are made.

# Seasonal and Interannual Variability in the Distribution and Removal of Terrigenous Dissolved Organic Carbon in the Amazon River Plume

Rachel P. Martineac<sup>1</sup>, Renato M. Castelao<sup>1</sup>, and Patricia M. Medeiros<sup>1</sup>

<sup>1</sup>Department of Marine Sciences, University of Georgia, Athens, GA, USA

**Abstract** The Amazon River is a large source of terrigenous dissolved organic carbon (tDOC) to the Atlantic Ocean. The fate of this tDOC in the ocean remains unclear despite its importance to the global carbon cycle. Here, we used two decades of satellite ocean color to describe variability in tDOC in the Amazon River plume. Our analyses showed that tDOC distribution has a distinct seasonal pattern, reaching northwest toward the Caribbean during high discharge periods, and moving eastward entrained in the North Brazil Current retroflection during low discharge periods. Elevated tDOC content extended beyond the shelfbreak in all months of the year, suggesting that cross-shelf carbon transport occurs year-round. Maximum variability was found at the plume core, where seasonality accounted for 40% of the total variance, while interannual variability accounted for 15% of the variance. Our results revealed a seasonal pattern in tDOC removal over the shelf with increased consumption in May when river discharge is high. Anomalies in tDOC removal over the shelf with respect to the seasonal cycle were significantly correlated with anomalies in tDOC concentration offshore of the shelfbreak with a lag of 30–40 days, so that anomalously high inshore tDOC removal was associated with anomalously low tDOC content offshore. This suggests that variability in the offshore transport of tDOC in the Amazon River plume is modulated by interannual changes in tDOC removal over the shelf.

Plain Language Summary The Amazon River is an important source of dissolved organic carbon (DOC) of terrigenous origin to the Atlantic Ocean. It is often difficult to characterize the distribution and variability of this material in the ocean due to the lack of high resolution in situ observations spanning long periods of time. Here, we used satellite observations of terrigenous DOC (tDOC) to describe the behavior of the plume at seasonal and interannual scales. Our analyses showed that enhanced tDOC content is observed offshore of the continental margin during all months of the year, extending toward the Caribbean during high river discharge conditions and eastward during low discharge conditions associated with variability in the large-scale circulation. Our results also revealed that tDOC removal over the shelf varies seasonally, being enhanced earlier in the year when river discharge is high. Anomalies in tDOC removal over the shelf are significantly correlated with anomalies in tDOC content offshore with a lag of 30–40 days, suggesting that the offshore transport of carbon is modulated by tDOC consumption over the shelf.

#### 1. Introduction

Riverine transport provides the largest delivery of organic matter from land to ocean (Hedges et al., 1997; Raymond & Spencer, 2015), supplying a quantity sufficient to support the turnover of dissolved organic carbon (DOC) throughout the ocean (Williams & Druffel, 1987). Estimates of riverine transport of terrigenous DOC (tDOC) to the ocean range from 0.17 Pg C yr<sup>-1</sup> (Dai et al., 2012) to 0.36 Pg C yr<sup>-1</sup> (Aitkenhead & McDowell, 2000), with many other estimates over the past 5 decades falling in between (e.g., Cai, 2011; Harrison et al., 2005; Ludwig et al., 1996; Meybeck, 1982; Seitzinger et al., 2005; S. V. Smith & Hollibaugh, 1993). The Amazon River alone is responsible for 12%–20% of the global riverine tDOC flux to the ocean (Meybeck, 1982; Moreira-Turcq et al., 2003; Raymond & Spencer, 2015; Richey et al., 1986).

Much remains to be learned about the fate of this terrigenous material in the ocean. Despite the large inputs, tDOC is thought to be altered over relatively short time scales (Benner & Opsahl, 2001; Hernes & Benner, 2003), with the coastal ocean serving as a major sink (Fichot & Benner, 2014; Hedges et al., 1997). The main mechanisms responsible for removing tDOC in the coastal ocean include microbial degradation, photochemical processes, and flocculation (Asmala et al., 2014; Hernes & Benner, 2003; Sholkovitz, 1978). In the northern Gulf of Mexico, for example, recent studies have shown that over half of the tDOC from the Mississippi-Atchafalaya River system is

MARTINEAC ET AL. 1 of 17

# **Global Biogeochemical Cycles**

10.1029/2023GB007995

mineralized along the margin each year (Fichot & Benner, 2014). Since it is likely that the terrigenous material will continue to be degraded as it is transported offshore, the fraction of terrigenous material exported from that continental margin is likely to be even smaller.

Despite intense removal occurring in many coastal regions, other studies have demonstrated that a substantial fraction of the tDOC from rivers can escape the continental margin (Medeiros et al., 2015; Seidel et al., 2015) and be transported to the open ocean (Medeiros et al., 2016). Terrigenous DOC has indeed been observed in the deep Atlantic and Pacific Oceans (Medeiros et al., 2016; Opsahl & Benner, 1997). In the Amazon River to ocean continuum, up to 75% of the tDOC delivered to the ocean by the river can be transported off the continental margin, particularly during high discharge conditions (Medeiros et al., 2015). Since the Amazon River discharge is predicted to increase in future climate scenarios (Manabe et al., 2004; Nohara et al., 2006), the delivery of tDOC to the ocean and the export from the coastal margin may increase even further.

Identifying the relative contribution of different factors that may drive tDOC variability in the Amazon River plume offshore of the shelfbreak is difficult because in situ observations are scarce in the region. DOC concentration and DOM composition at the Amazon River mouth have been shown to vary seasonally due to changes in hydrology and variations in source waters along the lower reach of the river, and as such the lability of the material exported to the shelf also varies seasonally (Seidel et al., 2016). The quantity and quality of the organic matter in the river that is exported to the shelf also varies on interannual scales in relation to climate variability (Kurek et al., 2021). Although previous studies have investigated tDOC degradation in the Amazon River and plume (e.g., Amon & Benner, 1996; Cao et al., 2016; Medeiros et al., 2015; Seidel et al., 2015, 2016; Ward et al., 2013), they only represent snapshots in time at a few locations, and thus cannot fully capture seasonal and interannual variability. Additionally, the transport of tDOC and other materials in the ocean often occurs in relatively narrow filaments that are easily missed by low-resolution in situ data (Strub et al., 1991). Remote sensing can help fill that gap by providing observations over a large span of the Amazon River plume for long periods of time.

Recent studies have shown that the spectral slope coefficient of chromophoric dissolved organic matter (CDOM) between 275 and 295 nm ( $S_{275-295}$ ) can be used as a tracer of tDOC in river-influenced ocean margins (Fichot & Benner, 2012; Fichot et al., 2014; Medeiros et al., 2017). Algorithms based on remote sensing reflectance (Rrs) data from the Moderate Resolution Imaging Spectroradiometer (MODIS) have been developed to estimate the spectral slope coefficient of CDOM absorbance from satellite ocean color data (Fichot et al., 2013, 2014). Fichot et al. (2014) showed that  $S_{275-295}$  from satellites agrees with in situ  $S_{275-295}$  measurements with an average uncertainty of 10%. By using a nonlinear regression to model the relationship between in situ  $S_{275-295}$  and tDOC concentration, estimates of tDOC content from ocean color can be obtained (Fichot et al., 2014).

Much has been learned about the Amazon River plume using satellite measurements of salinity (e.g., Fournier et al., 2015, 2017) and ocean color (Del Vecchio & Subramaniam, 2004; Fratantoni & Glickson, 2002; Gouveia, Gherardi, Wagner, et al., 2019; Longhurst, 1993; Molleri et al., 2010; Muller-Karger et al., 1988, 1995; Salisbury et al., 2011). Many of these previous studies relied on relatively short time series lasting only a few years, which makes it difficult to characterize plume variability at seasonal and/or lower frequencies. With almost 20 years of satellite observations of ocean color now available, we adapted and refined the algorithm developed by Fichot et al. (2013, 2014) to provide a detailed characterization of variability in the distribution of terrigenous DOC from the Amazon River in the Atlantic Ocean at seasonal and interannual scales. We also investigated tDOC removal over the Amazonian shelf, and its relation to tDOC variability offshore.

#### 2. Methods

#### 2.1. Study Area

Peak discharge from the main stem of the Amazon River occurs during May to June reaching an average maximum of  $\sim$ 240,000 m³ s¹, and discharge minima is historically experienced between November and December ( $\sim$ 80,000 m³ s¹; Richey et al., 1990; Lentz, 1995a). Interannual variability in river discharge is modulated by climate variability, with El Niño Southern Oscillation (ENSO) cycles being particularly important (Richey et al., 1989). As riverine water mixes with oceanic water, a plume of low-salinity water is formed spreading to the northwest along the shelf. The plume typically continues northwestward toward the Caribbean from January

MARTINEAC ET AL. 2 of 17

19449224, 2024, 6, Downloaded from https://agupubs.onlinelibrary.wiley.com/doi/10.1029/2023GB007995, Wiley Online Library on [19/08/2024]. See the Terms and Conditions

and-conditions) on Wiley Online Library for rules of use; OA articles are governed by the applicable Creative Commons Licens

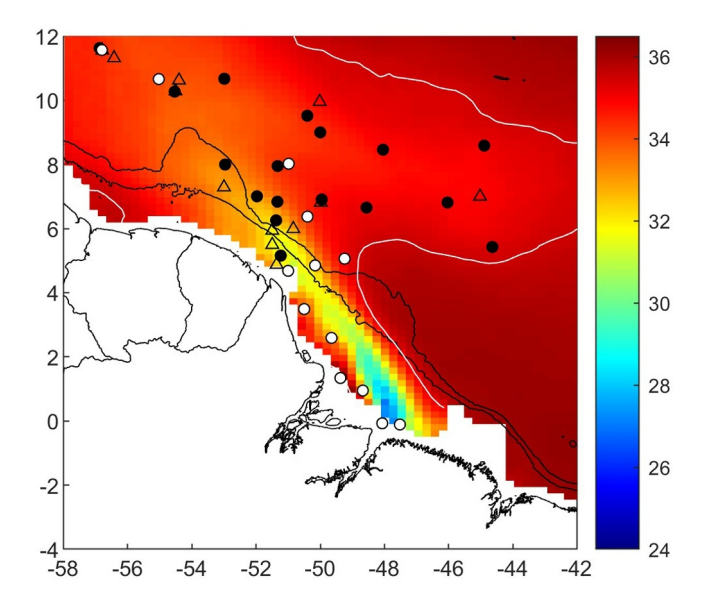


**Figure 1.** Long-term mean (January 2010 to December 2021) of sea surface salinity from Soil Moisture Ocean Salinity (SMOS) for the Amazon River plume and western tropical Atlantic Ocean. The 35.5 salinity contour is shown in white. Black contours are the 100 and 2,000 m isobaths. The locations of sample stations from research cruises in 2010, 2011, and 2012 are shown by triangles, black circles, and white circles, respectively. Note that optical data are not available for 2010.

through June, but it is predominantly deflected eastward from August to October entrained in the North Brazil Current (NBC) retroflection (Lentz, 1995a).

#### 2.2. In Situ Observations

In situ surface observations were collected in the Amazon River plume during three research cruises to the western tropical Atlantic Ocean, one in May/June 2010, one in September/October 2011 and another in July 2012 (Figure 1). Samples collected during May/June 2010 coincided with a high discharge period ( $\sim$ 300,000 m³ s<sup>-1</sup>) while those collected in September/October 2011 coincided with a low discharge period ( $\sim$ 110,000 m³ s<sup>-1</sup>). Sampling in July 2012 followed a record peak in river discharge (maximum of  $\sim$ 370,000 m³ s<sup>-1</sup>). Data collection and chemical analyses are described in detail in Medeiros et al. (2015), Seidel et al. (2015), and Cao et al. (2016), including DOC concentrations, bulk  $\delta$ <sup>13</sup>C ratios of DOC and S<sub>275–295</sub>. No optical data (S<sub>275–295</sub>) was collected during the May/June 2010 research cruise (Medeiros et al., 2015). The in situ concentration of tDOC was determined here as

$$[tDOC] = [DOC] \times f_{tDOC}$$
 (1)

where [DOC] and [tDOC] are the in situ DOC and tDOC concentrations, respectively, and  $f_{\text{tDOC}}$ 

$$f_{\text{tDOC}} = \frac{{}^{13}\text{C}_{\text{Sample}} - {}^{13}\text{C}_{\text{marine}}}{{}^{13}\text{C}_{\text{terrigenous}} - {}^{13}\text{C}_{\text{marine}}}$$
(2)

is the fraction of terrigenous DOC in the sample estimated using the  $\delta^{13}C$  measurements reported by Medeiros et al. (2015) for marine and terrigenous end members, as well as the sample value. The calculation was repeated 1,000 times varying endmember and sample values, so as to propagate uncertainties due to temporal variability in endmember values (as reported by Medeiros et al., 2015) and analytical variability. A nonlinear regression of the form (Fichot et al., 2014)

$$\ln([tDOC]) = \exp(\alpha - \beta \times S_{275-295}) + \exp(\gamma - \delta \times S_{275-295})$$
(3)

was used to parameterize the relationship between the in situ spectral slope measurements and the in situ tDOC concentrations estimated using Equation 1 in the Amazon River plume, where

$$\alpha = 4.083$$
,  $\beta = 280.382$ ,  $\gamma = 1.886$ , and  $\delta = 36.418$ .

This allowed tDOC to be estimated from  $S_{275-295}$  measurements (Figure 2a).

#### 2.3. Terrigenous DOC From Satellite Observations

We followed Fichot et al. (2014) to obtain satellite-derived estimates of spectral slope via log-linearized daily remote-sensing reflectance data,  $Rrs(\lambda)$  at  $\lambda = 443, 488, 555, 667$ , and 678 nm, from MODIS at 4-km resolution:

$$\ln(S_{275-295}) = \varepsilon + \zeta \times \ln(\text{Rrs}(443)) + \eta \times \ln(\text{Rrs}(448)) + \theta \times \ln(\text{Rrs}(555)) + \varphi \times \ln(\text{Rrs}(667)) + \chi$$
$$\times \ln(\text{Rrs}(678)) \tag{4}$$

where

 $\varepsilon = -3.1221$ ,  $\zeta = 0.0673$ ,  $\eta = 0.3266$ ,  $\theta = -0.07457$ ,  $\varphi = -0.4599$ , and  $\chi = 0.2917$  are the derived regression coefficients from Fichot et al. (2014). Data collection during the research cruises to the Amazon River plume did

MARTINEAC ET AL. 3 of 17

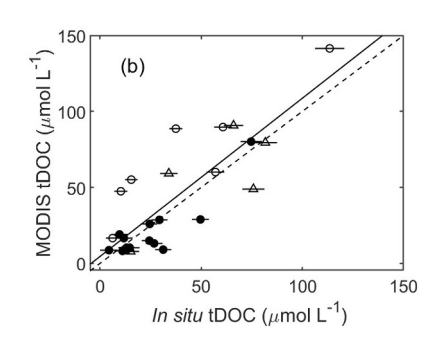


**Figure 2.** (a) Semi-log plot of the relationship between in situ measurements of the chromophoric dissolved organic matter (CDOM) spectral slope between 275 and 295 nm and in situ terrigenous dissolved organic carbon (tDOC) concentrations calculated using Equation 1. The black curve represents the nonlinear regression described in Equation 3. (b) The in situ point measurements of tDOC concentrations from Equation 1 were paired with 7-day averages of satellite-derived tDOC concentrations calculated using Equations 3 and 4. Dashed line is the 1:1 line. Linear regression is shown by solid black line. White circles, black circles, and white triangles represent data from 2012, 2011, and 2010, respectively. Error bars indicate uncertainty in the estimate of in situ tDOC from Equation 1 due to temporal variability in end members and analytical variability. Note that less data are shown in panel (b) than in panel (a) because Moderate Resolution Imaging Spectroradiometer (MODIS) observations are not always available for a match up with the in situ data due to cloud cover.

not include in situ data of Rrs. As such, we used the regression coefficients listed in Equation 4, which were derived by Fichot et al. (2014) using observations from the continental margin in the northern Gulf of Mexico under the influence of the Mississippi River plume. We note that a nonlinear regression with a form similar to Equation 4 but using slightly different coefficients was successfully used in the Arctic Ocean (Fichot et al., 2013). Furthermore, Fichot et al. (2014) noted that although region-specific parameterizations are always ideal, they applied the algorithm specifically developed for the Gulf of Mexico (Equation 4) to their Arctic Ocean data set (Fichot et al., 2013) for testing purposes (i.e., without re-calibrating it to the Arctic Ocean), which yielded accurate estimates of  $S_{275-295}$  (within  $\pm 10\%$  error). This led Fichot et al. (2014) to conclude that the algorithm should work well in other coastal environments under the influence of large tDOC inputs. Once maps of  $S_{275-295}$ were obtained for the Amazon River plume region based on MODIS data using Equation 4, satellite-derived estimates of tDOC could be obtained using Equation 3. Note that the coefficients used in Equation 3 were derived using observations from the Amazon River plume, since the relationship between optical properties and DOC concentrations often varies between regions (Mannino et al., 2008). Once obtained, satellite estimates of tDOC were compared with the in situ data. Comparisons between in situ and satellite-derived observations are always challenging, in part because in situ data represent a single location in space, while satellite observations represent averages over the satellite footprint size. Additionally, substantial gaps in data coverage are observed in the region in daily satellite observations due to cloud cover. To address this, we built 7-day averages of the satellite observations centered around the time of in situ data collection before comparing them with in situ measurements. This time scale is comparable to that used by Fichot et al. (2014), who binned the satellite data over 10-11 days before comparisons with in situ measurements. Despite these uncertainties, the 7-day averages of satellite-derived tDOC and the in situ point-measurements of tDOC from Equation 1 were found to be significantly correlated (Figure 2b; r = 0.83, p < 0.01; linear regression y = ax + b, with a = 1.04 and  $b = 4.56 \,\mu\text{mol L}^{-1}$ ; root-mean-square error = 20.3  $\mu$ mol L<sup>-1</sup>). The daily tDOC estimates from MODIS were then used to build monthly averages. This method has been shown to provide accurate estimates of tDOC concentrations in the Gulf of Mexico (Fichot et al., 2014) and in the Arctic Ocean (Fichot et al., 2013), suggesting that it can be applied successfully to other regions where optical data can be used to identify tDOC, such as the Amazon River plume (Cao et al., 2016).

Terrigenous DOC concentrations can vary substantially in the Amazon River plume and surrounding ocean. To better characterize the reach of enhanced tDOC in the region, we divided the number of months during which a pixel had tDOC concentrations larger than a given threshold by the total number of months with available data for that pixel during the study period, yielding a frequency of plume occurrence (Da Silva & Castelao, 2018). Visual inspection of the monthly tDOC distribution indicated that a threshold of  $10 \ \mu mol \ L^{-1}$  effectively delineated the boundary of the plume. Tests using a larger threshold of  $15 \ \mu mol \ L^{-1}$  yielded qualitatively similar results to those described here. To quantify intraseasonal, seasonal and interannual variability in tDOC content in the western

MARTINEAC ET AL. 4 of 17

19449224, 2024, 6, Downloaded from https://agupubs.onlinelibrary.wiley.com/doi/10.1029/2023GB007995, Wiley Online Library on [19/08/2024]. See the Terms

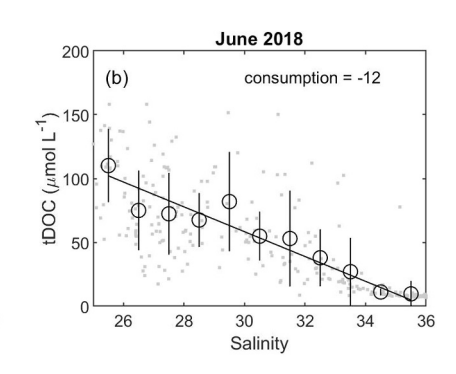


**Figure 3.** Scatter plots of surface salinity from Soil Moisture Ocean Salinity (SMOS) and terrigenous dissolved organic carbon (tDOC) from Moderate Resolution Imaging Spectroradiometer (MODIS) over the shelf (in area identified in Figure 9a) for salinity larger than 25 for two months as examples, (a) May 2010 and (b) June 2018. Gray dots represent comparison on a pixel-by-pixel basis, while large open circles represent bin averages, with error bars representing the standard deviation within each bin. Black solid line represents conservative mixing. Integrated deviations from conservative mixing are also listed (μmol L<sup>-1</sup> psu), with larger positive values suggesting larger tDOC removal over the shelf.

tropical Atlantic Ocean, we first low-pass filtered the monthly data using a 12-month filter (cosine-Lanczos filter; Mooers & Smith, 1968), which captured mostly interannual variability (Legaard & Thomas, 2006). The residue between the original time series and the low-pass filtered data includes variability at seasonal and higher frequencies. We then low-pass filtered the residue time series with a 6-month window to extract the seasonal signal. The new residue contains mostly intraseasonal variability. At each location, we followed Legaard and Thomas (2007) and approximated the total variance of the time series as the sum of the variances of the time series at the different frequency bands (i.e., intraseasonal, seasonal and interannual). The error associated with this assumption (i.e., the difference between the variance of the original data and the sum of the variances of the multiple time series for the different frequencies considered) is generally less than 15%.

Interannual variability in tDOC in regions off the shelf was investigated through an empirical orthogonal function (EOF) decomposition. Given that the Amazon River plume is strongly modulated by seasonality (e.g., Coles et al., 2013; Foltz et al., 2015; Fratantoni & Glickson, 2002; Lentz, 1995a; Muller-Karger et al., 1988), we first removed the seasonal cycle by removing the monthly averages of the tDOC concentrations from the time series. Although the residue time series still contains variability at seasonal scales (Chelton, 1982), this allows for better identification of interannual anomalies in the data set. Furthermore, we only considered observations from pixels offshore of the 2,000 m isobath, so that we could identify offshore areas characterized by large anomalies. Statistically significant EOF modes were identified following Overland and Preisendorfer (1982).

#### 2.4. Sea Surface Salinity

To track the temporal and spatial evolution of the Amazon River plume, satellite observations of sea surface salinity (SSS) were obtained from the Soil Moisture Ocean Salinity (SMOS; Boutin et al., 2022) mission. Observations are available since 2009. We used the Level 3 debiased version 7 product distributed by LOCEAN, which is made available on a 25-km grid every 4 days. The overall accuracy of 9-day composites of SMOS salinity data in tropical regions is of the order of 0.3 practical salinity units (psu; Fournier et al., 2015; Reul et al., 2014). SMOS has been successfully used previously to investigate salinity variability in the Amazon River plume (e.g., Gouveia, Gherardi, Wagner, et al., 2019; Grodsky et al., 2014) as well as to identify variations in the offshore advection of plume waters (Fournier et al., 2017).

#### 2.5. tDOC Removal Over the Shelf

In order to obtain a measure of tDOC removal over the shelf, we used 30-day averages of SSS and tDOC from satellite observations to identify deviations from conservative mixing. Analyses were restricted to 2010–2021, when both SSS and tDOC were available simultaneously. Specifically, we made scatter plots of bin-averages of SSS versus tDOC over the shelf, downstream of the Amazon River mouth. Examples for 2 months are shown in Figure 3. The black solid line indicates conservative mixing between two end members, assuming that tDOC =  $0 \, \mu mol \, L^{-1}$  for a salinity of 36 psu, and tDOC =  $350 \, \mu mol \, L^{-1}$  at the river mouth. This value was chosen

MARTINEAC ET AL. 5 of 17

based on the average tDOC concentration measured at the river mouth by Medeiros et al. (2015) and Seidel et al. (2016). For each 30-day period, we integrated the difference between the bin-averaged pairs of SSS and tDOC and the conservative mixing line for salinity values larger than 25 psu, yielding an integrated deviation from conservative mixing ( $\mu$ mol L<sup>-1</sup> psu; we pursued the integration such that tDOC consumption is positive). That integrated deviation is related to the amount of tDOC removal over the shelf. Large deviations, as in Figure 3a, are consistent with more degradation and/or flocculation, while small values are consistent with less degradation. To account for variability in tDOC concentration at the river mouth, we repeated the calculations described above 1,000 times but varying the tDOC concentration at the river mouth used in the end-member computation each time by up to  $\pm 12\%$ . Lastly, instead of using a fixed value as the tDOC concentration at the river mouth (i.e.,  $350 \pm 12\%$   $\mu$ mol L<sup>-1</sup>), we also pursued a second set of calculations imposing a seasonal cycle in tDOC concentrations at the river mouth, with an amplitude of 50  $\mu$ mol L<sup>-1</sup> peaking in June (Araujo et al., 2014). As described above, those calculations were also repeated 1,000 times, varying the tDOC concentration at the river mouth for each month in the seasonal cycle by up to  $\pm 12\%$ .

#### 3. Results

In the plume region, in situ observations of  $\delta^{13}$ C and surface salinity reported by Medeiros et al. (2015) and Seidel et al. (2015) were found to be highly correlated (r=0.88, p<0.001), with  $\delta^{13}$ C signatures being depleted in riverine samples ( $\sim$ -29.3 to -30%) and enriched in the most oceanic samples ( $\sim$ -21.8 to -22.4%). Calculated fractions of the terrigenous portion of surface DOC based on in situ samples and obtained through Equation 1 ranged from 0% to 3% at the distal portion of the plume to 40%-60% on-shelf, approaching 100% near the river mouth (estimates have an uncertainty of about  $\pm 5\%$  points). This is consistent with Medeiros et al. (2015) analyses, who used a two end-member mass balance based on Fourier transform ion cyclotron resonance mass spectrometry data to show that on-shelf plume waters were characterized by DOC with 40%-60% of terrigenous content.

#### 3.1. tDOC Variability in the Amazon River Plume

Monthly averages of tDOC concentrations (Figure 4) and frequency of plume occurrence (Da Silva & Castelao, 2018) based on tDOC data (Figure 5) revealed marked variability between months. From December to February, tDOC concentrations within the 100 m isobath were comparatively small (Figure 4), and high frequencies of plume occurrence were mostly found over the shelf, extending off the shelf to the northwest (Figure 5). tDOC concentrations over the shelf increased from March to May (Figure 4) as the Amazon River discharge also increased (Richey et al., 1990), with the plume extending beyond the continental margin toward the Caribbean 60%–90% of the time (Figure 5). However, the frequency of plume occurrence remained quite small to the east. Concentrations began to slowly decrease from June to August over the shelf, and the plume extended progressively eastward during that period under the influence of the NBC retroflection (Coles et al., 2013; Fratantoni et al., 1995; Garzoli et al., 2004; Johns et al., 1990). This is consistent with Lentz (1995a), who used historical in situ salinity observations to show that the freshest water in the retroflection region is observed in July and August. Even though tDOC concentrations were low in the NBC retroflection area compared to the shelf, the frequency of plume occurrence was high, exceeding 80% (Figure 5). The frequency of plume occurrence in the northwest toward the Caribbean decreased to around 50% during that time. From August to November, the signature of the retroflection on tDOC concentration and plume distribution was still clearly visible but it decreased progressively, and by December, large tDOC concentrations were once again mostly restricted to shelf waters (Figures 4 and 5).

The previous analysis indicated that substantial variability is observed in tDOC concentration and/or in the spatial distribution of the area under the influence of tDOC-enriched waters. That is expected, given that the Amazon River plume experiences substantial seasonal variability (e.g., Fournier et al., 2015; Lentz, 1995a; Lentz & Limeburner, 1995). A large range in salinity variability was observed in the core of the plume (Figure 6a). Even though the influence of tDOC from the Amazon River was felt over the shelf in all months during the study period (Figure 5), tDOC concentrations were quite variable, experiencing a large maximum range of  $\sim$ 200  $\mu$ mol L<sup>-1</sup> inshore of the 100 m isobath (Figure 6b). These variations may be related to variations in the volume of freshwater and in the amount of tDOC exported from the Amazon River, but also due to shifts in the position of the plume associated with winds or other forcings (Fournier et al., 2017). Previous studies have observed shifts in the salinity plume core throughout the year, most recently observing a tight nearshore plume in March-May and then moving

MARTINEAC ET AL. 6 of 17

19449224, 2024, 6, Downloaded from https://agupubs.onlinelibrary.wiley.com/doi/10.1029/2023GB007995, Wiley Online Library on [19/08/2024]. See the Terms and Conditions (https://onlinelibrary.wiley.

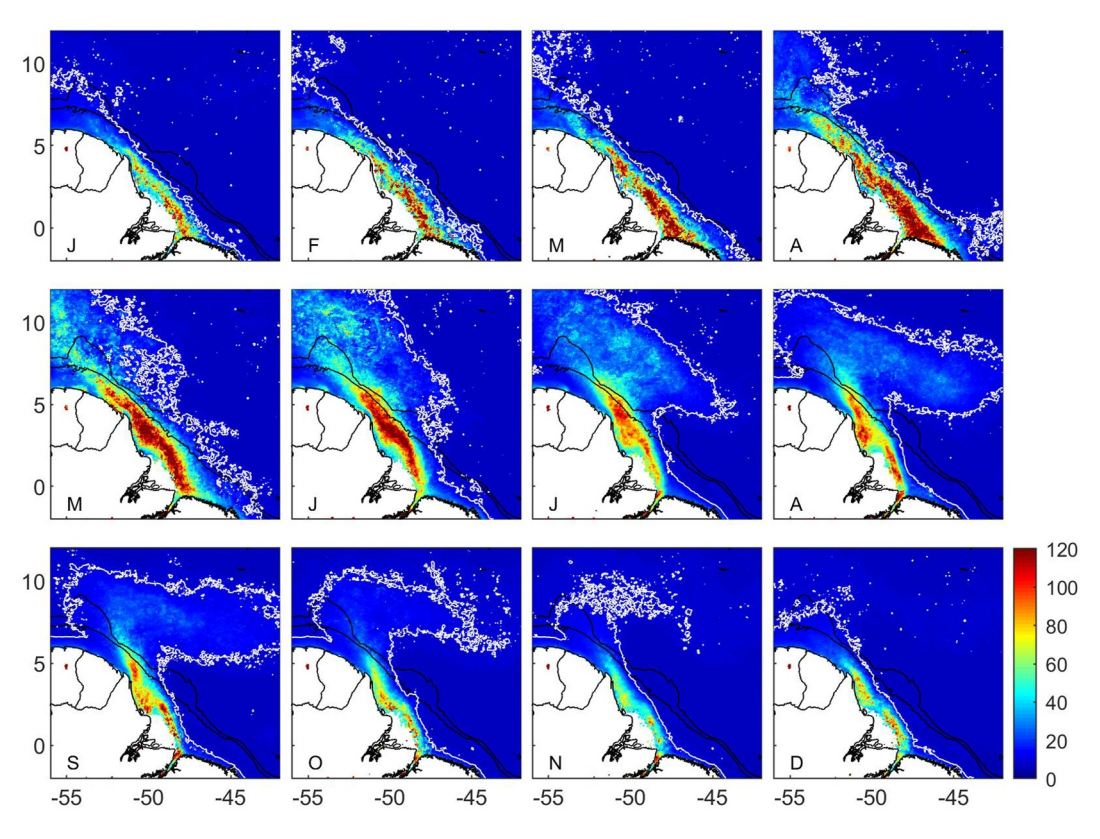


Figure 4. Monthly averages of terrigenous dissolved organic carbon (tDOC) concentration ( $\mu$ mol L<sup>-1</sup>). The tDOC = 10  $\mu$ mol L<sup>-1</sup> contour is shown in white. Black contours are the 100 and 2,000 m isobaths. Months are indicated on the bottom left corner of each panel.

offshore  $\sim$ 75 km during June-August (Ruault et al., 2020). Enhanced variability was also observed in the NBC retroflection region, although substantially smaller than over the shelf (Figure 6).

One goal of this study was to investigate variability in tDOC content in regions off the shelf and to later relate it to tDOC removal over the shelf (in Section 3.2). Given that estimating removal involved comparing tDOC and SSS observations, we restricted the analysis to the time period when both sets of observations were available simultaneously. The first EOF mode of the tDOC anomalies (i.e., with the seasonal cycle removed) offshore of the 2,000 m isobath explained 12.2% of the total variance (Figure 7a), and it is characterized by a large signature offshore to the north of French Guiana, extending from the 2,000 m isobath to around  $12^{\circ}N$ . The amplitude time series revealed that the mode is dominated by an event in June 2014 (Figure 7c), indicating increased tDOC content offshore (i.e., in the region with positive EOF values in Figure 7a) during that time. This followed exceptionally intense wet conditions in 2014 austral summer, when rainfall measured  $\sim 100\%$  higher than average (Espinoza et al., 2013). Fournier et al. (2017) used observations from SMOS to show that low-salinity waters in the core of the plume extended far beyond the shelfbreak in June 2014 (see their Figure 9), approximately coinciding with the area captured by the EOF mode (areas in red in Figure 7a).

The second EOF mode explained 7.1% of the total variance (Figure 7b), and it is also characterized by enhanced values just offshore of the shelfbreak, but with an out-of-phase response to the east and to the west of  $\sim 51^{\circ}$ W. In the region with enhanced signature to the east of  $51^{\circ}$ W, where EOF 2 is positive, the mode explains as much as 30% of the local variance (not shown). In that region, the EOF analyses revealed that tDOC anomalies were enhanced (in comparison with the seasonal cycle) when the amplitude time series (Figure 7d) is positive, such as in mid-2012 and for several months in 2021, and depleted when the amplitude time series is negative, such as in mid-2013 and mid-2015. The opposite is true for the region to the west of  $51^{\circ}$ W, where EOF 2 is negative. EOF 2 explained less than 15% of the local variance at that location (note that this region spatially overlaps with the region with an enhanced signature in EOF 1).

MARTINEAC ET AL. 7 of 17

19449224, 2024, 6, Downloaded from https://agupubs.onlinelibrary.wiley.com/doi/10.1029/2023GB007995, Wiley Online Library on [19/08/2024]. See the Terms and Conditions (https://onlinelibrary.wiley.com/doi/10.1029/2023GB007995, Wiley Online Library on [19/08/2024]. See the Terms and Conditions (https://onlinelibrary.wiley.com/doi/10.1029/2023GB007995, Wiley Online Library on [19/08/2024]. See the Terms and Conditions (https://onlinelibrary.wiley.com/doi/10.1029/2023GB007995, Wiley Online Library on [19/08/2024]. See the Terms and Conditions (https://onlinelibrary.wiley.com/doi/10.1029/2023GB007995, Wiley Online Library on [19/08/2024]. See the Terms and Conditions (https://onlinelibrary.wiley.com/doi/10.1029/2023GB007995, Wiley Online Library on [19/08/2024]. See the Terms and Conditions (https://onlinelibrary.wiley.com/doi/10.1029/2023GB007995, Wiley Online Library on [19/08/2024]. See the Terms and Conditions (https://onlinelibrary.wiley.com/doi/10.1029/2023GB007995, Wiley Online Library on [19/08/2024]. See the Terms and Conditions (https://onlinelibrary.wiley.com/doi/10.1029/2023GB007995, Wiley Online Library on [19/08/2024]. See the Terms and Conditions (https://onlinelibrary.wiley.com/doi/10.1029/2023GB007995, Wiley Online Library on [19/08/2024]. See the Terms and Conditions (https://onlinelibrary.wiley.com/doi/10.1029/2023GB007995, Wiley Online Library on [19/08/2024]. See the Terms and Conditions (https://onlinelibrary.wiley.com/doi/10.1029/2023GB007995, Wiley Online Library on [19/08/2024]. See the Terms and Conditions (https://onlinelibrary.wiley.com/doi/10.1029/2023GB007995, Wiley Online Library on [19/08/2024]. See the Terms and Conditions (https://onlinelibrary.wiley.com/doi/10.1029/2023GB007995, Wiley Online Library on [19/08/2024]. See the Terms and Conditions (https://onlinelibrary.wiley.com/doi/10.1029/2023GB007995, Wiley Online Library.wiley.com/doi/10.1029/2023GB007996, Wiley Online Library.wiley.com/doi/10.1029/2023GB007996, Wiley Online Library.wiley.com/doi/10.1029/2023GB007996, Wiley Onli

and-conditions) on Wiley Online Library for rules of use; OA articles are governed by the applicable Creative Commons License

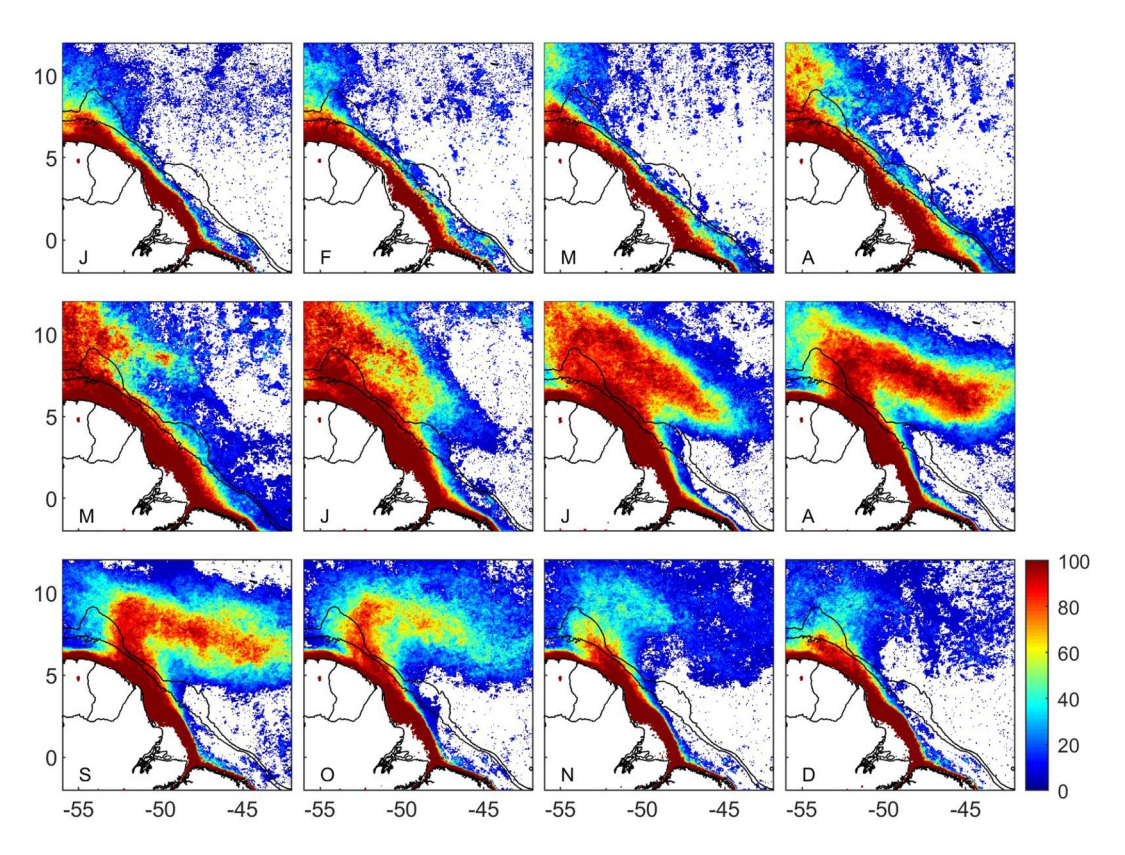


Figure 5. Frequency of plume occurrence (ratio of the number of observations with terrigenous dissolved organic carbon (tDOC) >  $10 \,\mu$ mol L<sup>-1</sup> at a given pixel and the number of valid observations at that pixel times  $100 \,\text{to}$  yield a percentage) for each month. Zero frequency is shown in white. Black contours are the  $100 \,\text{and} \, 2,000 \,\text{m}$  isobaths. Months are indicated on the bottom left corner of each panel.

Lastly, we computed the relative contribution of variability at the interannual, seasonal and intraseasonal frequency bands to the total variance in tDOC at each pixel (Figure 8). Note that missing observations precluded the analyses in some pixels, and that a different scale was used on the colorbar of the right panel. Although there were several gaps in the observations, it is possible to see that the contribution of seasonal variability was increased over the shelf and in the retroflection region, reaching ~40% (Figure 8b). The largest variances were observed in the intraseasonal band (Figure 8c). This indicates that variability at short time scales, such as due to shifts in the position of the plume associated with wind forcing (e.g., Fournier et al., 2017) or due to meanders and eddies (e.g., Fratantoni & Glickson, 2002), dominated tDOC variance in the region. Interannual variability, on the other hand, accounted for 10%–15% of the total variance over the shelf and in the retroflection region (Figure 8a).

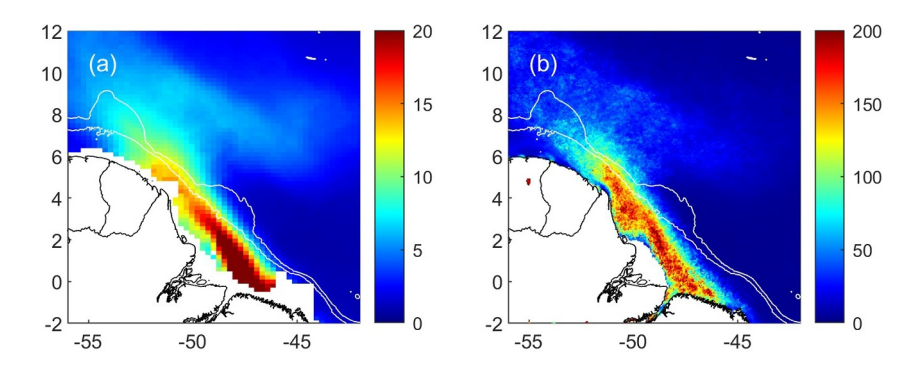
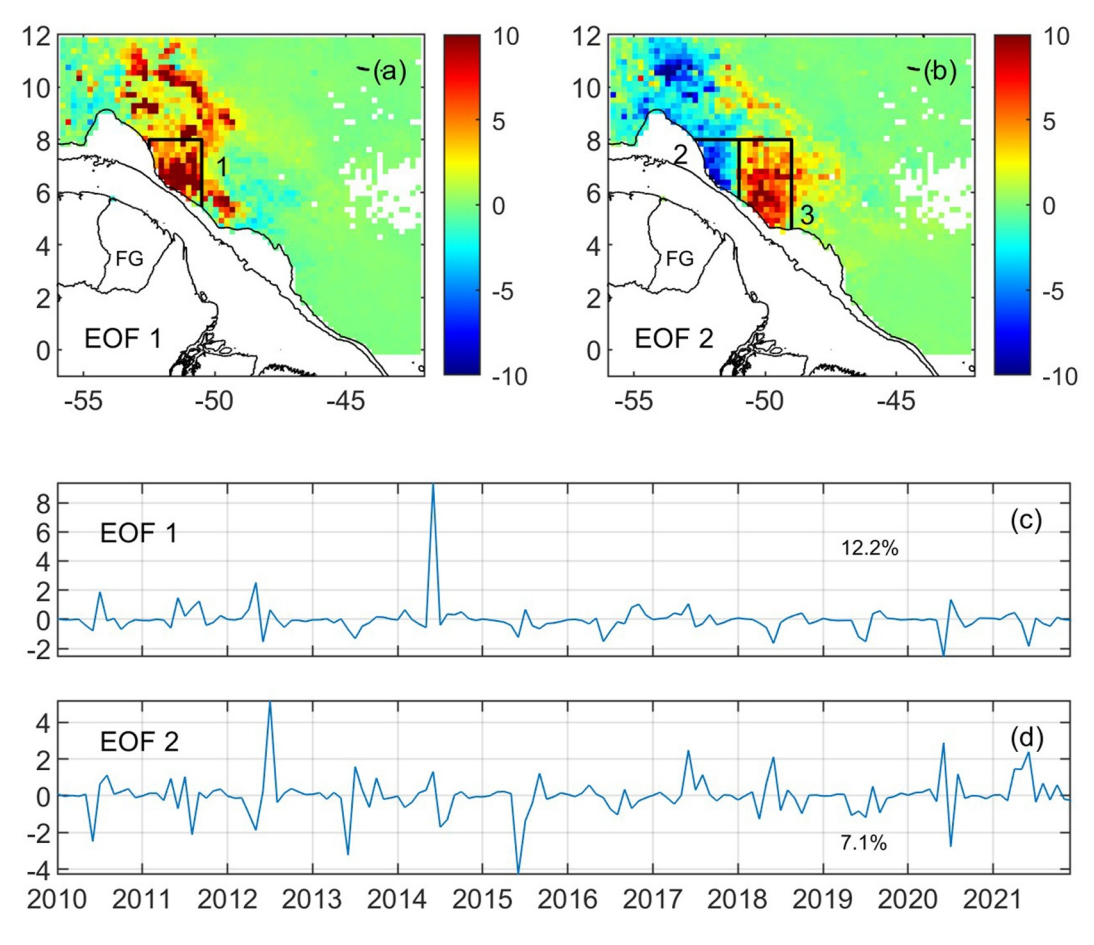


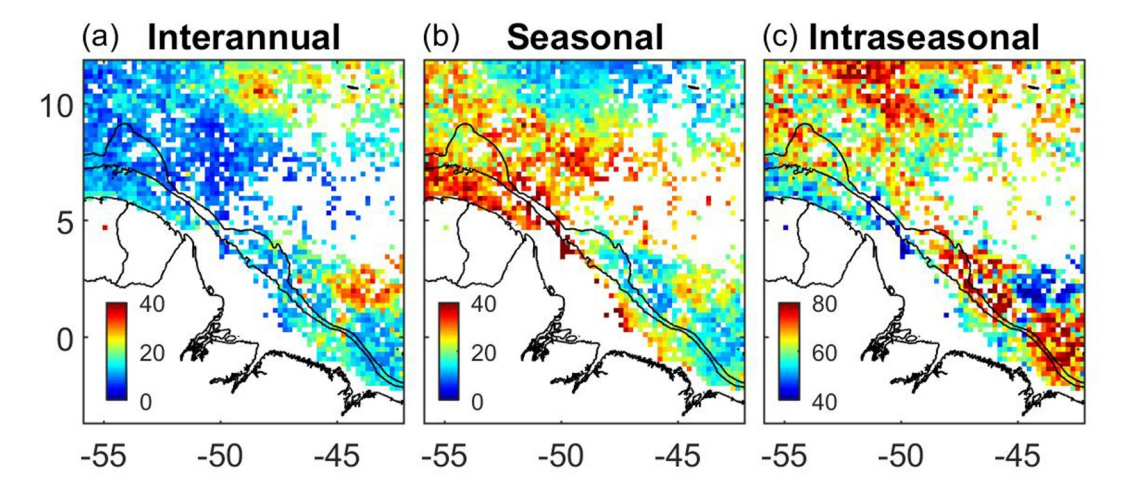
Figure 6. Range of (a) salinity (psu) and (b) terrigenous dissolved organic carbon (tDOC) concentration ( $\mu$ mol  $L^{-1}$ ) variability at each pixel. White contours are the 100 and 2,000 m isobaths.

MARTINEAC ET AL. 8 of 17

19449224, 2024, 6, Downloaded from https://agupubs.onlinelibrary.viley.com/doi/10.1029/2023GB007995, Wiley Online Library on [19/08/2024]. See the Terms and Conditions (https://onlinelibrary.viley.com/terms-and-conditions) on Wiley Online Library for rules of use; OA articles are governed by the applicable Creative Commons Licensea

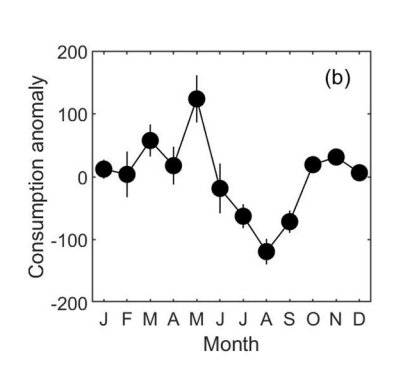


**Figure 7.** (a) Empirical orthogonal function (EOF) 1 and (b) EOF 2 of terrigenous dissolved organic carbon (tDOC) variability offshore of the 2,000 m isobath with seasonal cycle removed. The 100 and 2,000 m isobaths are shown. Areas 1, 2, and 3 as referenced in the text are denoted. The amplitude time series for EOF 1 and EOF 2 are shown in panels (c) and (d), respectively. The fraction of variance explained by each mode is also shown. FG: French Guiana.



**Figure 8.** Fraction of total variance (%) explained by (a) interannual, (b) seasonal, and (c) intraseasonal variability. Color bar scale on the right panel is different to better reveal spatial patterns. Black contours are the 100 and 2,000 m isobaths.

MARTINEAC ET AL. 9 of 17



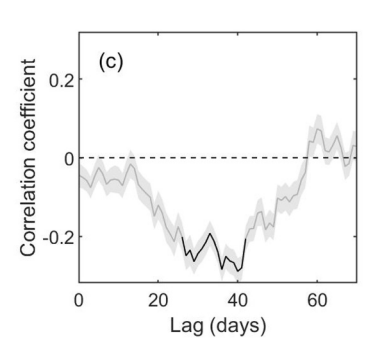


Figure 9. (a) Sea surface salinity (SSS) from Soil Moisture Ocean Salinity (SMOS) on 23 May 2011. Small black dots indicate areas where SSS and terrigenous dissolved organic carbon (tDOC) data were compared to estimate tDOC removal over the shelf (see text for details; note that region close to shore with high salinity is excluded). (b) Monthly averages of tDOC consumption anomaly ( $\mu$ mol L<sup>-1</sup> psu) in the area identified in panel (a) after removing the long-term average. Examples for 2 months are shown in Figure 3. Positive values indicate larger consumption than the long-term average. (c) Correlation coefficient between time series of spatially averaged tDOC anomalies offshore (in area 3 in Figure 7b) and time series of tDOC removal anomalies over the shelf (in area identified in panel (a) by small black dots). The seasonal cycle was removed from both time series. Negative correlations indicate that increased removal over the shelf is associated with negative tDOC anomalies offshore. The light shaded area indicates the range in correlations for each lag obtained by varying the tDOC concentration at the river mouth used in end member computation by up to  $\pm 12\%$ . The calculation was repeated 1,000 times. Statistically significant correlations (at the 95% level) in at least 80% of the repetitions are shown in black. Correlations were computed based on 30-day averages for different lags. A lag of 1 day indicates that the spatially averaged tDOC anomaly offshore from 1 June 2010 to 30 June 2010, for example, was compared with the tDOC removal anomaly over the shelf from 31 May 2010 to 29 June 2010, and so forth.

#### 3.2. tDOC Variability Offshore: The Importance of tDOC Removal Over the Shelf

Variability in tDOC content offshore of the shelfbreak in the Amazon River plume likely depends on a variety of processes, including variability in the DOC flux at the river mouth as well as transport and chemical/biological transformation processes. With the EOF decompositions described above, we identified regions offshore of the shelfbreak characterized by large increases or decreases in tDOC content compared to the seasonal cycle (areas in red or blue in Figures 7a and 7b). Here, we attempted to quantify tDOC removal over the shelf, as well as its implications for tDOC variability in those offshore regions. To obtain an integrated measure of tDOC degradation over the shelf, we compared 30-day averages of SSS and tDOC observations over the shelf (in the area shown in Figure 9a) and conservative mixing between the two end members. Instances when tDOC behaved conservatively (e.g., in June 2018; Figure 3b) are consistent with the material being resistant to degradation, while large differences from conservative mixing (e.g., in May 2010; Figure 3a) are consistent with tDOC removal (e.g., microbial-, photo-degradation, flocculation) or the presence of additional water masses. It could also be related to transformations that change the organic matter in such a way that tDOC would be missed using our approach. There was considerable scatter in the relation between SSS and tDOC on a pixel-by-pixel level in the two examples shown in Figure 3, possibly related to uncertainties in the satellite observations (see discussion section for details). Despite this, there was a clear tendency for tDOC concentrations to be lower than the conservative mixing line in May 2010, while in June 2018, tDOC concentrations more closely matched conservative mixing. The analysis was repeated for all months from 2010 to 2021, when both SSS and tDOC observations were available simultaneously. Monthly averages of the time series of deviations from conservative mixing (with the long-term average removed) for 2010-2021 presented clear seasonal changes, suggesting enhanced tDOC removal early in the year peaking in May when river discharge is generally high, and reduced removal later in the year, especially in August and September (Figure 9b).

It is reasonable to assume that changes in tDOC removal over the shelf may influence tDOC content offshore. To quantify whether enhanced tDOC removal over the shelf can result in negative tDOC anomalies offshore, while periods where tDOC over the shelf behaves conservatively are followed by positive tDOC anomalies offshore, we compared time series of tDOC content offshore with time series of tDOC removal over the shelf (i.e., the time series of integrated deviations from conservative mixing). Time series of tDOC anomalies offshore were computed by spatially averaging observations for the three regions identified in Figure 7, namely the area with

MARTINEAC ET AL. 10 of 17

large positive EOF 1 values in Figure 7a and the areas with large positive and negative EOF 2 values in Figure 7b. Before computing correlations, we first removed the monthly averages from both time series since both surface salinity (e.g., Fournier et al., 2015) and tDOC (Figure 4) are characterized by a strong seasonal cycle. Additionally, it is reasonable to expect that there should be a time lag between any possible impact of tDOC removal anomaly over the shelf and tDOC anomalies offshore. Therefore, we computed multiple time series of tDOC removal anomaly (i.e., time series of integrated deviations from conservative mixing with the seasonal cycle removed) over the shelf for lags of up to 70 days. A lag of 0 days indicates that the spatially averaged tDOC anomaly (seasonal cycle removed) offshore from 1 June 2010 to 30 June 2010, for example, was compared with tDOC removal anomaly (seasonal cycle removed) over the shelf during the same period. For a lag of 1 day, the same spatially averaged tDOC anomaly offshore was compared with tDOC removal anomaly over the shelf from 31 May 2010 to 29 June 2010, and so forth. For areas 1 and 2 (shown in Figure 7), no statistically significant correlations were observed. For area 3, where EOF 2 explained as much as 30% of the local variance, the time series were also found to be uncorrelated for small lags of up to 15 days and for lags larger than about 50 days (Figure 9c). However, correlation coefficients were negative and increased in magnitude for intermediate lags. For lags between 26 and 42 days, correlation coefficients were statistically significant (at the 95% level), hovering around -0.2 to -0.3. This supports the hypothesis that negative tDOC anomalies offshore can be associated with prior increases in tDOC removal over the shelf. Repeating the analysis but imposing a seasonal cycle in tDOC concentrations at the river mouth used as endmember when computing the integrated measure of tDOC removal over the shelf yielded results consistent with those reported here in Figure 9c.

#### 4. Discussion

The fate of terrigenous material in the ocean is of fundamental importance. Many previous studies have indicated that coastal zones act as sinks of tDOC, with the organic material being efficiently and rapidly removed in ocean margins (e.g., Fichot & Benner, 2014; Hedges et al., 1997; Hernes & Benner, 2003). Notwithstanding, analyses at the molecular level have suggested that much of the Amazon River DOC is surprisingly stable in the coastal ocean, with 50%–76% of the tDOC delivered to the ocean by the river being transported beyond the continental margin (Medeiros et al., 2015). Medeiros et al. (2015) observed larger transport during high discharge conditions and relatively smaller transport during low flow conditions, suggesting that continued intensification of the hydrological cycle (Gouveia, Gherardi, & Aragão, 2019; Marengo et al., 2011) could result in increased offshore transport of tDOC in future climate scenarios. Their analysis was based on in situ observations during a few research cruises to the Amazon River plume, and as such, they were not able to investigate temporal variability in the transport other than during those expeditions.

Our study builds on several previous studies that have characterized the Amazon River plume and its variability using in situ observations (e.g., Lentz, 1995a, 1995b) and satellite measurements of salinity (e.g., Fournier et al., 2015, 2017) and ocean color (Del Vecchio & Subramaniam, 2004; Fratantoni & Glickson, 2002; Gouveia, Gherardi, Wagner, et al., 2019; Longhurst, 1993; Molleri et al., 2010; Muller-Karger et al., 1988, 1995; Salisbury et al., 2011). Several of these previous studies have used satellite imagery of chlorophyll, diffuse attenuation coefficient at 490 nm, or the absorption coefficient of colored detrital matter at the reference wavelength 443 nm  $(a_{\text{cdm}})$  to track the position of the plume. Here, we used an algorithm (Fichot et al., 2013, 2014) specifically designed to track the terrigenous component of the DOC pool, providing a link between limited and expensive in situ measurements and increasingly available satellite data. MODIS observations are now available for almost 2 decades, and the use of a longer time series allows for quantifying tDOC variability in the Amazon River plume over broad areas off the shelf. We also identified the evolution of the frequency of plume occurrence (Da Silva & Castelao, 2018) based on tDOC observations. That is an important metric because it reveals how often a specific location is under the influence of plume waters (which are typically enriched in nutrients and other substances) in each month. The presence of plume waters can influence a variety of biogeochemical processes, such as primary productivity stimulated by nutrients (Gouveia, Gherardi, Wagner, et al., 2019; W. O. Smith & Demaster, 1996) and the related CO<sub>2</sub> drawdown (e.g., Chen et al., 2012; Ibánhez et al., 2015; Körtzinger, 2003) associated with phytoplankton blooms (W. O. Smith & Demaster, 1996). It can also influence light availability (Del Vecchio & Subramaniam, 2004). Our observations reveal that the distribution of tDOC is consistent with previous characterizations of the plume core movement based on salinity data, with three main dispersal patterns: (a) a narrow band of flow along the northeastern South American coast from December to March; (b) flow to the Caribbean region between April and June; and (c) flow to the Central Equatorial Atlantic Ocean with plume waters entrained

MARTINEAC ET AL. 11 of 17

in the NBC retroflection from July to November (e.g., Curtin, 1986; Del Vecchio & Subramaniam, 2004; Lentz & Limeburner, 1995; Molleri et al., 2010; Salisbury et al., 2011; Varona et al., 2019). Elevated tDOC content extended beyond the shelfbreak in some capacity in all months of the year, suggesting that cross-shelf carbon transport occurs year-round. Even though tDOC concentrations were comparatively low in the retroflection region, our novel estimates of the frequency of plume occurrence were quite high, exceeding 80% from July to September. The seasonal evolution of the plume accounted for as much as 40% of the total variance in tDOC concentrations over the shelf and in the retroflection. The long-term time series also allowed us to quantify interannual variability, something that has been difficult to achieve in previous studies due to the use of comparatively short time series lasting only a few years. Interannual variability accounted for ~15% of the total variance in most locations. EOF decompositions of tDOC data with the seasonal cycle removed revealed several instances of large variability in tDOC off the shelf, with large increases in specific years.

SSS and optical properties in the plume have been shown to be strongly correlated to each other (Fournier et al., 2015), but considerable deviation from conservative mixing has been reported. Salisbury et al. (2011) noted that negative anomalies indicating degradation of colored detrital matter (which includes absorption by both particulate detritus and CDOM) were often observed in the distal areas of the plume and suggested that they were related to photochemical oxidation. This motivated our current attempt to quantify tDOC removal over the shelf, and to relate it to tDOC variability off the shelf. Despite noise in the data, our comparisons of SSS and tDOC have indicated a clear seasonal pattern in tDOC removal over the shelf, with increased removal occurring early in the year when river discharge is increasing and approaching its seasonal peak. This is consistent with observations in other systems. Off coastal Georgia, U.S., for example, Letourneau and Medeiros (2019) showed that DOC utilization at the mouth of the Altamaha River was correlated with river discharge, increasing during peak river flow. Increased DOC losses have also been observed in Artic rivers during the spring freshet, both due to biological and photochemical pathways (Mann et al., 2012). Although a large fraction of the dissolved molecules of terrigenous origin are respired in the Amazon River by microbes before export to the coastal ocean (Ward et al., 2013), incubations of water collected near the Amazon River mouth have indicated that bio- and photo-transformations can still alter up to 30% of the DOM molecular formulae (Seidel et al., 2016). Flocculation can also contribute to the removal of tDOC (Khoo et al., 2022). These are consistent with the statistically significant alterations in tDOC content observed here over the shelf after export from the river.

The time series of monthly anomalies (i.e., seasonal cycle removed) in tDOC removal over the shelf was found to be significantly correlated negatively with anomalies in tDOC concentration in an area off the shelf, offshore of the 2,000 m isobath, peaking for lags of about 30-40 days. Although correlation coefficients are small, ranging in magnitude from 0.2 to 0.3, they are significant at the 95% confidence level. Additionally, the change in correlation coefficients as a function of lag suggested that the analysis is robust: (a) Correlations coefficients are small for short lags as expected, since tDOC removal over the shelf would not immediately lead to tDOC variability offshore due to the time it takes for the water to be transported offshore; (b) Coefficients are also small for large lags far exceeding the residence time over the shelf; (c) Coefficients are largest in magnitude for lags of about 30-40 days, which approximately coincide with the time it takes for drifters released near the river mouth to leave the shelf (i.e., <30–60 days) (Coles et al., 2013; Limeburner et al., 1995), as they are entrained in the energetic and swift NBC (Coles et al., 2013). We note that one important driver of tDOC variability offshore is likely to be variability in the tDOC flux at the river mouth. As captured by Medeiros et al. (2015) mass balance approach, the largest offshore transport of tDOC occurs during peak discharge conditions, being reduced during low discharge conditions. Our results suggest, however, that interannual variability in the fraction of the tDOC that escapes the shelf and may be entrained in the large-scale circulation is likely to be modulated by interannual changes in tDOC removal over the shelf (Figure 10). We note that tDOC removal by salt-induced flocculation may result in the production of particulate matter (e.g., Khoo et al., 2022), which could still escape the continental shelf.

Although the correlation coefficients found here are significant (Figure 9c), they are not high, consistent with the idea that other factors are important in controlling tDOC variability offshore. Another related candidate for influencing tDOC variability off the shelf is variations in ocean circulation. Variations in the spatial extent of the plume offshore have been linked to river discharge, ocean rainfall, advection, wind forcing and turbulent mixing (e.g., Coles et al., 2013; Grodsky et al., 2014; Hu et al., 2004; Molleri et al., 2010). The containment of plume waters closer to the coast versus increased off-shelf advection has been shown to be more closely related to eddy-driven transport and cross-shore winds than to interannual variability in river discharge (Fournier et al., 2017). The strength of surface currents over the shelf is likely to be particularly important for the offshore transport of

MARTINEAC ET AL. 12 of 17

19449224, 2024, 6, Downloaded from https://agupubs.onlinelibrary.wiley.com/doi/10.1029/2023GB007995, Wiley Online Library on [19/08/2024]. See the Terms and Conditions (https://agupubs.onlinelibrary.wiley.com/doi/10.1029/2023GB007995, Wiley Online Library on [19/08/2024]. See the Terms and Conditions (https://agupubs.onlinelibrary.wiley.com/doi/10.1029/2023GB007995, Wiley Online Library on [19/08/2024]. See the Terms and Conditions (https://agupubs.onlinelibrary.wiley.com/doi/10.1029/2023GB007995, Wiley Online Library on [19/08/2024]. See the Terms and Conditions (https://agupubs.onlinelibrary.wiley.com/doi/10.1029/2023GB007995, Wiley Online Library on [19/08/2024]. See the Terms and Conditions (https://agupubs.com/doi/10.1029/2023GB007995, Wiley Online Library.wiley.com/doi/10.1029/2023GB007995, Wiley Online Library.

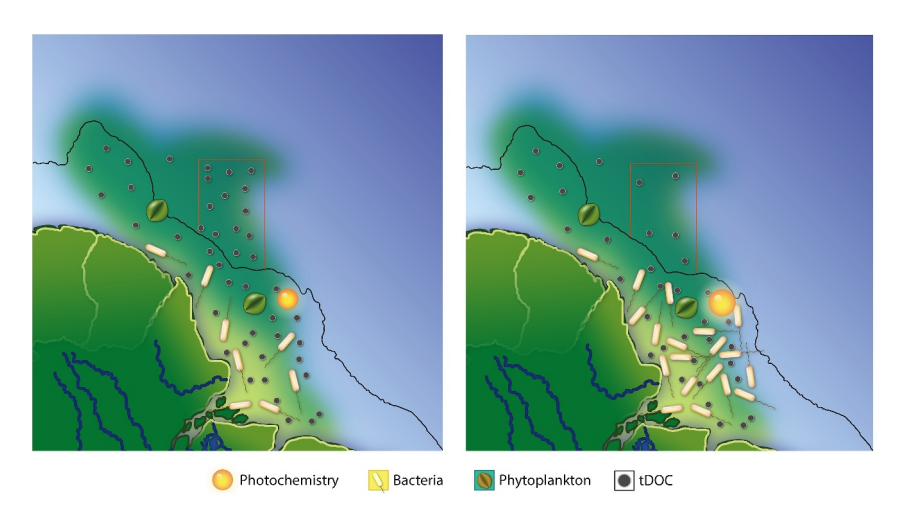


**Figure 10.** Schematic representation of modulation in the offshore transport of terrigenous dissolved organic carbon (tDOC) in the Amazon River plume. When tDOC removal processes over the shelf are anomalously small, anomalously large tDOC concentrations are found offshore of the 2,000 m isobath (left panel). However, when removal processes over the shelf are increased, less tDOC can escape the shelf (right panel). tDOC removal processes can include biodegradation, photochemical reactions, and flocculation. Medeiros et al. (2015) results suggest that biodegradation is likely to play a key role over the shelf. Black contour denotes the 2,000 m isobath. Symbols are representative of bacterial degradation and photochemical reactions, while small circles represent the multiple components of the tDOC pool. Red lines delineate the area offshore of the 2,000 m isobath where the correlation between tDOC removal over the shelf and anomalies in concentration offshore are the highest.

tDOC. In particular, intensifications in coastal currents in comparison to the seasonal pattern would presumably lead to short residence times over the shelf and increased offshore transport. As such, it would be interesting to compare some metric of the intensity of coastal currents over the shelf that extends for several years with tDOC variability offshore. We attempted to use surface currents from the Ocean Surface Current Analysis Real-time (OSCAR) data product (Bonjean & Lagerloef, 2002) for that purpose, but data over the shelf are often missing, not allowing for robust comparisons. It may be possible to use surface drifter trajectories acquired from the Global Drifter Program (Hansen & Poulain, 1996) to obtain measures of variability in the transit time between the river mouth and the shelf break. Coles et al. (2013) analyzed drifter trajectories from 1979 to 2011 near the Amazon River mouth and noted that the temporal and spatial distribution of surface drifters were not uniform. Furthermore, they noted that a substantial fraction of the available drifters ran aground near the river mouth, leaving only 72 trajectories for their analysis. This suggests that outputs from a well-calibrated ocean model may be needed to help identify the role of variability in shelf circulation on tDOC anomalies offshore.

Our comparisons between in situ and MODIS tDOC data suggest that the algorithm may overestimate tDOC concentrations in some instances, such as in 2012 for example, (Figure 2b). It is not clear if conditions were different during that period, resulting in a systematic bias, or if the pattern is simply a result of few match ups being available for comparison between in situ and satellite data (due to differences in cloud cover, less match ups were available for 2012 compared to 2011). There are many sources of uncertainties in the analysis pursued here. Biases of the order of 0.3-0.5 psu between in situ and SMOS salinity observations have been reported in the region, with the standard deviation of the in situ and satellite SSS differences increasing to 1 psu in plume waters (Fournier et al., 2015). Direct comparisons between SMOS and MODIS data, as done for estimating deviations from conservative mixing, are made more uncertain by the intrinsic differences in the characteristics of the data sets. SMOS and MODIS have different footprint sizes, and MODIS imagery cannot be obtained in cloudy conditions. Additionally, SMOS surface salinity measurements are representative of the top few centimeters of the ocean (Boutin et al., 2016), while MODIS observations are representative of the first few meters (first optical depth). There are also uncertainties associated with ocean color algorithms, which are expected to have increased errors over the shelf and especially closer to the river mouth due to high sediment concentrations (Salisbury et al., 2011). Phytoplankton growth has been observed in all but the most turbid areas of the river plume (e.g., DeMaster et al., 1996; Hulburt & Corwin, 1969; Subramaniam et al., 2008). Biological activity has been shown to increase in the northwestern part of the plume during summer (Westberry et al., 2008). Large phytoplankton

MARTINEAC ET AL. 13 of 17



## **Global Biogeochemical Cycles**

10.1029/2023GB007995

blooms and associated changes in ocean color could result in errors in the estimate of tDOC. Phytoplankton has been shown to change the DOM composition in the Amazon River plume by adding new compounds to the DOM pool (Medeiros et al., 2015). As these newly added compounds are remineralized, they could potentially modify the CDOM pool (e.g., Boss et al., 2001; Nelson et al., 1998; Twardowski & Donaghay, 2001; Yamashita & Tanoue, 2004), potentially modifying our satellite-based estimates of spectral slope even if there are no changes in the terrigenous component of the DOC. Future studies are needed to investigate if those uncertainties associated with sediment concentrations and/or phytoplankton blooms would only add noise to the data, or if they could result in higher or lower estimates of tDOC concentrations, and to further refine the algorithm used here. Despite all these sources of uncertainties, our satellite estimates compared favorably with in situ tDOC measurements. It is also encouraging that the analyses captured a seasonal pattern in tDOC removal that is consistent with that observed in other systems (e.g., Letourneau & Medeiros, 2019; Mann et al., 2012), and that anomalies (i.e., deviations from the seasonal cycle) in tDOC removal over the shelf explain some of the variability in tDOC anomalies offshore with a lag consistent with the average shelf residence time.

#### 5. Conclusions

We used two decades of observations to characterize seasonal and interannual variability in the distribution of tDOC in the western tropical Atlantic Ocean under the influence of the Amazon River plume. The analyses revealed that water with high terrigenous carbon content is transported beyond the continental margin during all months of the year, where it may be entrained in the large-scale ocean circulation. We also estimated removal of the terrigenous organic matter over the shelf, likely due to a combination of microbial and photochemical processes and flocculation. tDOC removal in the Amazon shelf is characterized by a clear seasonal cycle consistent with variability in river discharge. Furthermore, anomalies in tDOC content offshore are related to anomalies in tDOC removal over the shelf, indicating that removal processes over the Amazonian shelf play a significant role in controlling carbon export from the continental margin (Figure 10). Changes in the hydrological cycle have been observed worldwide and are predicted to increase in future climate scenarios (Manabe et al., 2004; Nohara et al., 2006), suggesting that coastal systems under the influence of large rivers may also experience substantial changes. The approach used here can be used to monitor and quantify those changes as well as to investigate the controls of tDOC variability in other coastal margins characterized by large tDOC inputs.

#### **Conflict of Interest**

The authors declare no conflicts of interest relevant to this study.

#### **Data Availability Statement**

The data used in this study are publicly available at oceandata.sci.gsfc.nasa.gov/directdataaccess (MODIS Rrs) and www.catds.fr/Products/Available-products-from-CEC-OS/CEC-Locean-L3-Debiased-v7 (SMOS SSS). In situ data used can be found in Medeiros et al. (2015).

#### References

Aitkenhead, J. A., & McDowell, W. H. (2000). Soil C:N ratio as a predictor of annual riverine DOC flux at local and global scales. *Global Biogeochemical Cycles*, 14(1), 127–138. https://doi.org/10.1029/1999GB900083

Amon, R. M. W., & Benner, R. (1996). Bacterial utilization of different size classes of dissolved organic matter. Limnology & Oceanography, 41(1), 41–51. https://doi.org/10.4319/lo.1996.41.1.0041

Araujo, M., Noriega, C., & Lefèfre, N. (2014). Nutrients and carbon fluxes in the estuaries of major rivers flowing into the tropical Atlantic. Frontiers in Marine Science, 1, 1–10. https://doi.org/10.3389/fmars.2014.00010

Asmala, E., Bowers, D. G., Autio, R., Kaartokallio, H., & Thomas, D. N. (2014). Qualitative changes of riverine dissolved organic matter at low salinities due to flocculation. *Journal of Geophysical Research: Biogeosciences*, 119(10), 1919–1933. https://doi.org/10.1002/2014JG002722

Benner, R., & Opsahl, S. (2001). Molecular indicators of the sources and transformations of dissolved organic matter in the Mississippi River plume. *Organic Geochemistry*, 32(4), 597–611. https://doi.org/10.1016/s0146-6380(00)00197-2

Bonjean, F., & Lagerloef, G. S. (2002). Diagnostic model and analysis of the surface currents in the tropical Pacific Ocean. *Journal of Physical Oceanography*, 32(10), 2938–2954. https://doi.org/10.1175/1520-0485(2002)032<2938:dmaaot>2.0.co;2

Boss, E., Pegau, W. S., Zaneveld, J. R. V., & Barnard, A. H. (2001). Spatial and temporal variability of absorption by dissolved material at a continental shelf. *Journal of Geophysical Research*, 106(C5), 9499–9507. https://doi.org/10.1029/2000jc900008

Boutin, J. Y., Chao, W. E., Asher, T., Delcroix, R., Drucker, K., Drushka, N., et al. (2016). Satellite and in situ salinity: Understanding near-surface stratification and subfootprint variability. *Bulletin of the American Meteorological Society*, 97(8), 1391–1407. https://doi.org/10.1175/bams-d-15-00032.1

#### Acknowledgments

The authors acknowledge the two anonymous reviewers and the editors for their thoughtful and constructive comments and suggestions, which resulted in an improved manuscript. This manuscript has also benefited from discussions with M.A. Moran and A.C. Spivak (U. Georgia). This work was partially supported by the National Science Foundation (OCE-2219874).

MARTINEAC ET AL. 14 of 17



## **Global Biogeochemical Cycles**

- 10.1029/2023GB007995
- Boutin, J. Y., Vergely, J.-L., & Khvorostyanov, D. (2022). SMOS SSS L3 maps generated by CATDS CEC LOCEAN. Debias V7.0. SEANOE. https://doi.org/10.17882/52804#91742
- Cai, W. J. (2011). Estuarine and coastal ocean carbon paradox: CO<sub>2</sub> sinks or sites of terrestrial carbon incineration? Annual Review of Marine Science, 3(1), 123–145, https://doi.org/10.1146/annurev-marine-120709-142723
- Cao, F., Medeiros, P. M., & Miller, W. L. (2016). Optical characterization of dissolved organic matter in the Amazon River plume and the Adjacent Ocean: Examining the relative role of mixing, photochemistry, and microbial alterations. *Marine Chemistry*, 186, 178–188. https://doi.org/10.1016/j.marchem.2016.09.007
- Chelton, D. (1982). Large-scale response of the California current to forcing by the wind stress curl. In California cooperative oceanic fisheries investigations report (Vol. 119, pp. 130–148).
- Chen, C.-T. A., Huang, T.-H., Fu, Y.-H., Bai, Y., & He, X. (2012). Strong sources of CO<sub>2</sub> in upper estuaries become sinks of CO<sub>2</sub> in large river plumes. Current Opinion in Environmental Sustainability, 4(2), 179–185. https://doi.org/10.1016/j.cosust.2012.02.003
- Coles, V. J., Brooks, M. T., Hopkins, J., Stukel, M. R., Yager, P. L., & Hood, R. R. (2013). The pathways and properties of the Amazon River plume in the tropical north Atlantic Ocean. *Journal of Geophysical Research: Oceans*, 118(12), 6894–6913. https://doi.org/10.1002/ 2013ic008981
- Curtin, T. B. (1986). Physical observations in the plume region of the Amazon River during peak discharge—II. Water masses. *Continental Shelf Research*, 6(1–2), 53–57. https://doi.org/10.1016/0278-4343(86)90053-1
- Dai, M., Yin, Z., Meng, F., Liu, Q., & Cai, W.-J. (2012). Spatial distribution of riverine DOC inputs to the ocean: An updated global synthesis. Current Opinion in Environmental Sustainability, 4(2), 170–178. https://doi.org/10.1016/j.cosust.2012.03.003
- Da Silva, C. E., & Castelao, R. M. (2018). Mississippi River plume variability in the Gulf of Mexico from SMAP and MODIS-Aqua observations. Journal of Geophysical Research: Oceans, 123(9), 6620–6638. https://doi.org/10.1029/2018JC014159
- Del Vecchio, R., & Subramaniam, A. (2004). Influence of the Amazon River on the surface optical properties of the western tropical north Atlantic Ocean. *Journal of Geophysical Research*, 109, C11. https://doi.org/10.1029/2004jc002503
- DeMaster, D. J., Smith, W., Nelson, D. M., & Aller, J. Y. (1996). Biogeochemical processes in Amazon shelf waters: Chemical distributions and uptake rates of silicon, carbon and nitrogen. Continental Shelf Research, 16(5–6), 617–643. https://doi.org/10.1016/0278-4343(95)00048-8
- Espinoza, J. C., Ronchail, J., Frappart, F., Lavado, W., Santini, W., & Guyot, J. L. (2013). The major floods in the Amazonas River and tributaries (western Amazon basin) during the 1970–2012 period: A focus on the 2012 flood. *Journal of Hydrometeorology*, 14(3), 1000–1008. https://doi.org/10.1175/jhm-d-12-0100.1
- Fichot, C. G., & Benner, R. (2012). The spectral slope coefficient of chromophoric dissolved organic matter (S<sub>275-295</sub>) as a tracer of terrigenous dissolved organic carbon in river-influenced ocean margins. *Limnology & Oceanography*, 57(5), 1453–1466. https://doi.org/10.4319/lo.2012. 57.5.1453
- Fichot, C. G., & Benner, R. (2014). The fate of terrigenous dissolved organic carbon in a river-influenced ocean margin. *Global Biogeochemical Cycles*, 28(3), 300–318. https://doi.org/10.1002/2013GB004670
- Fichot, C. G., Kaiser, K., Hooker, S., Amon, R., Babin, M., Belanger, S., et al. (2013). Pan-Arctic distributions of continental runoff in the Arctic Ocean. Scientific Reports, 3(1), 1053. https://doi.org/10.1038/srep01053
- Fichot, C. G., Lohrenz, S. E., & Benner, R. (2014). Pulsed, cross-shelf export of terrigenous dissolved organic carbon to the Gulf of Mexico. Journal of Geophysical Research: Oceans, 119(2), 1176–1194. https://doi.org/10.1002/2013jc009424
- Foltz, G. R., Schmid, C., & Lumpkin, R. (2015). Transport of surface freshwater from the equatorial to the subtropical north Atlantic Ocean. Journal of Physical Oceanography, 45(4), 1086–1102. https://doi.org/10.1175/JPO-D-14-0189.1
- Fournier, S., Chapron, B., Salisbury, J., Vandemark, D., & Reul, N. (2015). Comparison of spaceborne measurements of sea surface salinity and colored detrital matter in the Amazon plume. *Journal of Geophysical Research: Oceans*, 120(5), 3177–3192. https://doi.org/10.1002/2014JC010109
- Fournier, S., Vandemark, D., Gaultier, L., Lee, T., Jonsson, B., & Gierach, M. M. (2017). Interannual variation in offshore advection of Amazon-Orinoco plume waters: Observations, forcing mechanisms, and impacts. *Journal of Geophysical Research: Oceans*, 122(11), 8966–8982. https://doi.org/10.1002/2017JC013103
- Fratantoni, D. M., & Glickson, D. A. (2002). North Brazil current ring generation and evolution observed with SeaWiFS. *Journal of Physical Oceanography*, 32(3), 1058–1074. https://doi.org/10.1175/1520-0485(2002)032<1058:nbcrga>2.0.co;2
- Fratantoni, D. M., Johns, W. E., & Townsend, T. L. (1995). Rings of the North Brazil Current: Their structure and behavior inferred from observations and a numerical simulation. *Journal of Geophysical Research*, 100(C6), 10633–10654. https://doi.org/10.1029/95jc00925
- Garzoli, S. L., Ffield, A., Johns, W. E., & Yao, Q. (2004). North Brazil Current retroflection and transports. *Journal of Geophysical Research*, 109(C1), C01013. https://doi.org/10.1029/2003JC001775
- Gouveia, N. A., Gherardi, D. F. M., & Aragão, L. E. O. C. (2019). The role of the Amazon River Plume on the intensification of the hydrological cycle. Geophysical Research Letters, 46(21), 12221–12229. https://doi.org/10.1029/2019g1084302
- Gouveia, N. A., Gherardi, D. F. M., Wagner, F. H., Paes, E. T., Coles, V. J., & Aragão, L. E. O. C. (2019). The salinity structure of the Amazon River Plume drives spatiotemporal variation of oceanic primary productivity. *Journal of Geophysical Research: Biogeoscience*, 124(1), 147–165. https://doi.org/10.1029/2018jg004665
- Grodsky, S. A., Reverdin, G., Carton, J. A., & Coles, V. J. (2014). Year-to-year salinity changes in the Amazon plume: Contrasting 2011 and 2012 Aquarius/SACD and SMOS satellite data. Remote Sensing of Environment, 140, 14–22. https://doi.org/10.1016/j.rse.2013.08.033
- Hansen, D. V., & Poulain, P.-M. (1996). Quality control and interpolations of WOCE-TOGA drifter data. Journal of Atmospheric and Oceanic Technology, 13(4), 900–909. https://doi.org/10.1175/1520-0426(1996)013<0900:qcaiow>2.0.co;2
- Harrison, J. A., Caraco, N., & Seitzinger, S. P. (2005). Global patterns and sources of dissolved organic matter export to the coastal zone: Results from a spatially explicit, global model. *Global Biogeochemical Cycles*, 19(4), GB4S04. https://doi.org/10.1029/2005gb002480
- Hedges, J. I., Keil, R. G., & Benner, R. (1997). What happens to terrestrial organic matter in the ocean? *Organic Geochemistry*, 27(5–6), 195–212. https://doi.org/10.1016/S0146-6380(97)00066-1
- Hernes, P. J., & Benner, R. (2003). Photochemical and microbial degradation of dissolved lignin phenols: Implications for the fate of terrigenous dissolved organic matter in marine environments. *Journal of Geophysical Research*, 108(C9), 3291. https://doi.org/10.1029/2002JC001421
- Hu, C., Montgomery, E. T., Schmitt, R. W., & Müller-Karger, F. E. (2004). The dispersal of the Amazon and Orinoco river water in the tropical Atlantic and Caribbean sea: Observation from space and S-PALACE floats. *Deep Sea Research Part II: Topical Studies in Oceanography*, 51(10–11), 1151–1171. https://doi.org/10.1016/s0967-0645(04)00105-5
- Hulburt, E. M., & Corwin, N. (1969). Influence of the Amazon River Outflow on the ecology of the western tropical Atlantic. III. The planktonic Flora between the Amazon River and the Windward Islands. *ICES Journal of Marine Science*, 55–72.
- Ibánhez, J. S. P., Diverrès, D., Araujo, M., & Lefèvre, N. (2015). Seasonal and interannual variability of sea-air CO<sub>2</sub> fluxes in the tropical Atlantic affected by the Amazon River plume. Global Biogeochemical Cycles, 29(10), 1640–1655. https://doi.org/10.1002/2015gb005110

MARTINEAC ET AL. 15 of 17

- Johns, W. E., Lee, T. N., Schott, F. A., Zantopp, R. J., & Evans, R. H. (1990). The North Brazil Current retroflection: Seasonal structure and eddy variability. *Journal of Geophysical Research*, 95(C12), 22103–22120. https://doi.org/10.1029/JC095iC12p22103
- Khoo, C. L. L., Sipler, R. E., Fudge, A. R., Beheshti Foroutani, M., Boyd, S. G., & Ziegler, S. E. (2022). Salt-induced flocculation of dissolved organic matter and iron is controlled by their concentration and ratio in boreal coastal systems. *Journal of Geophysical Research: Biogeosciences*, 127(11), e2022JG006844. https://doi.org/10.1029/2022JG006844
- Körtzinger, A. (2003). A significant CO<sub>2</sub> sink in the tropical Atlantic Ocean associated with the Amazon River plume. Geophysical Research Letters, 30, 24. https://doi.org/10.1029/2003g1018841
- Kurek, M. R., Stubbins, A., Drake, T. W., Moura, J. M. S., Holmes, R. M., Osterholz, H., et al. (2021). Drivers of organic molecular signatures in the Amazon River. Global Biogeochemical Cycles, 35(6), e2021GB006938. https://doi.org/10.1029/2021GB006938
- Legaard, K. R., & Thomas, A. C. (2006). Spatial patterns in seasonal and interannual variability of chlorophyll and sea surface temperature in the California Current. *Journal of Geophysical Research*, 111(C6), C06032. https://doi.org/10.1029/2005JC003282
- Legaard, K. R., & Thomas, A. C. (2007). Spatial patterns of intraseasonal variability of chlorophyll and sea surface temperature in the California Current. *Journal of Geophysical Research*, 112(C9), C09006. https://doi.org/10.1029/2007JC004097
- Lentz, S. J. (1995a). Seasonal variations in the horizontal structure of the Amazon plume inferred from historical hydrographic data. *Journal of Combusical Research*, 100(C2), 2301–2400, https://doi.org/10.1009/041C01347
- Geophysical Research, 100(C2), 2391–2400. https://doi.org/10.1029/94JC01847
  Lentz, S. J. (1995b). The Amazon River Plume during AMASSEDS: Subtidal current variability and the importance of wind forcing. Journal of
- Geophysical Research, 100(C2), 2377–2390. https://doi.org/10.1029/94JC00343
  Lentz, S. J., & Limeburner, R. (1995). The Amazon River Plume during AMASSEDS: Spatial characteristics and salinity variability. Journal of
- Geophysical Research, 100(C2), 2355–2375. https://doi.org/10.1029/94jc01411

  Letourneau, M. L., & Medeiros, P. M. (2019). Dissolved organic matter composition in a Marsh-dominated Estuary: Response to seasonal forcing and to the passage of a Hurricane. Journal of Geophysical Research: Biogeoscience, 124(6), 1545–1559. https://doi.org/10.1029/
- 2018JG004982
  Limeburner, R., Beardsley, R. C., Soares, I. D., Lentz, S. J., & Candela, J. (1995). Lagrangian flow observations of the Amazon River discharge into the North Atlantic. *Journal of Geophysical Research*, 100(C2), 2401–2415. https://doi.org/10.1029/94jc03223
- Longhurst, A. (1993). Seasonal cooling and blooming in tropical oceans. *Deep Sea Research Part I: Oceanographic Research Papers*, 40(11–12), 2145–2165. https://doi.org/10.1016/0967-0637(93)90095-k
- Ludwig, W., Probst, J., & Kempe, S. (1996). Predicting the oceanic input of organic carbon by continental erosion. *Global Biogeochemical Cycles*, 10(1), 23–41. https://doi.org/10.1029/95GB02925
- Manabe, S., Milly, P. C. D., & Wetherald, R. T. (2004). Simulated long-term change in river discharge and soil moisture due to global warming. Hydrological Sciences Journal, 49(4), 625–642. https://doi.org/10.1623/hysj.49.4.625.54429
- Mann, P. J., Davydova, A., Zimov, N., Spencer, R. G. M., Davydov, S., Bulygina, E., et al. (2012). DOM composition and lability during the Arctic spring freshet on the river Kolyma, Northeast Siberia. *Journal of Geophysical Research*, 117(G1), G01028. https://doi.org/10.1029/ 2011JG001798
- Mannino, A., Russ, M. E., & Hooker, S. B. (2008). Algorithm development and validation for satellite-derived distributions of DOC and CDOM in the U.S. Middle Atlantic Bight. *Journal of Geophysical Research*, 113(C7), C07051. https://doi.org/10.1029/2007JC004493
- Marengo, J. A., Tomasella, J., Alves, L. M., Soares, W. R., & Rodriguez, D. A. (2011). The drought of 2010 in the context of historical droughts in the Amazon region. *Geophysical Research Letters*, 38, 12. https://doi.org/10.1029/2011gl047436
- Medeiros, P. M., Babcock-Adams, L., Seidel, M., Castelao, R. M., Di Iorio, D., Hollibaugh, J. T., & Dittmar, T. (2017). Export of terrigenous dissolved organic matter in a broad continental shelf. Limnology & Oceanography, 62(4), 1718–1731. https://doi.org/10.1002/lno.10528
- Medeiros, P. M., Seidel, M., Niggemann, J., Spencer, R. G. M., Hernes, P. J., Yager, P. L., et al. (2016). A novel molecular approach for tracing terrigenous dissolved organic matter into the deep ocean. *Global Biogeochemical Cycles*, 30(5), 689–699. https://doi.org/10.1002/2015gb005320
- Medeiros, P. M., Seidel, M., Ward, N. D., Carpenter, E. J., Gomes, H. R., Niggemann, J., et al. (2015). Fate of the Amazon River dissolved organic matter in the tropical Atlantic Ocean. *Global Biogeochemical Cycles*, 29(5), 677–690. https://doi.org/10.1002/2015gb005115
- Meybeck, M. (1982). Carbon, nitrogen, and phosphorus transport by world rivers. American Journal of Science, 282(4), 401–450. https://doi.org/10.2475/ais.282.4.401
- Molleri, G. S. F., Novo, E. M. L. D. M., & Kampel, M. (2010). Space-time variability of the Amazon River plume based on satellite ocean color. Continental Shelf Research. 30(3-4), 342–352. https://doi.org/10.1016/j.csr.2009.11.015
- Mooers, C. N. K., & Smith, R. L. (1968). Continental shelf waves off Oregon. *Journal of Geophysical Research*, 73(2), 549–557. https://doi.org/10.1029/JB073i002p00549
- Moreira-Turcq, P., Seyler, P., Guyot, J. L., & Etcheber, H. (2003). Exportation of organic carbon from the Amazon River and its main tributaries. Hydrological Processes, 17(7), 1329–1344. https://doi.org/10.1002/hyp.1287
- Muller-Karger, F. E., McClain, C., & Richardson, P. (1988). The dispersal of the Amazon's water. *Nature*, 333(6168), 56–59. https://doi.org/10.1038/333056a0
- Muller-Karger, F. E., Richardson, P. L., & Mcgillicuddy, D. (1995). On the offshore dispersal of the Amazon's Plume in the North Atlantic: Comments on the paper by A. Longhurst, "Seasonal cooling and blooming in tropical oceans". *Deep Sea Research Part 1: Oceanographic Research Papers*, 42(11–12), 2127–2137. https://doi.org/10.1016/0967-0637(95)00085-2
- Nelson, N. B., Siegel, D. A., & Michaels, A. F. (1998). Seasonal dynamics of colored dissolved material in the Sargasso Sea. *Deep Sea Research Part I: Oceanographic Research Papers*, 45(6), 931–957. https://doi.org/10.1016/S0967-0637(97)00106-4
- Nohara, D., Kitoh, A., Hosaka, M., & Oki, T. (2006). Impact of climate change on river discharge projected by multimodel ensemble. *Journal of Hydrometeorology*, 7(5), 1076–1089. https://doi.org/10.1175/jhm531.1
- Opsahl, S., & Benner, R. (1997). Distribution and cycling of terrigenous dissolved organic matter in the ocean. *Nature*, 386(6624), 480–482. https://doi.org/10.1038/386480a0
- Overland, J. E., & Preisendorfer, R. W. (1982). A significance test for principal components applied to a cyclone climatology. *Monthly Weather Review*, 110(1), 1–4. https://doi.org/10.1175/1520-0493(1982)110
- Raymond, P. A., & Spencer, R. G. M. (2015). Chapter 11—Riverine DOM. In D. A. Hansell & C. A. Carlson (Eds.), Biogeochemistry of marine dissolved organic matter (2nd ed., pp. 509–533). Academic Press. Retrieved from https://www.sciencedirect.com/science/article/pii/ B978012405940500011X
- Reul, N., Fournier, S., Boutin, J., Hernandez, O., Maes, C., Chapron, B., et al. (2014). Sea surface salinity observations from space with the SMOS satellite: A new means to monitor the marine branch of the water cycle. *Surveys in Geophysics*, 35(3), 681–722. https://doi.org/10.1007/s10712-013-9244-0

MARTINEAC ET AL. 16 of 17

- Richey, J. E., Hedges, J. I., Devol, A. H., Quay, P. D., Victoria, R., Martinelli, L., & Forsberg, B. R. (1990). Biogeochemistry of carbon in the Amazon River. Limnology & Oceanography, 35(2), 352–371. https://doi.org/10.4319/lo.1990.35.2.0352
- Richey, J. E., Meade, R. H., Salati, E., Devol, A. H., Nordin, C. F., Jr., & Santos, U. D. (1986). Water discharge and suspended sediment concentrations in the Amazon River: 1982–1984. Water Resources Research, 22(5), 756–764. https://doi.org/10.1029/wr022i005p00756
- Richey, J. E., Nobre, C., & Deser, C. (1989). Amazon River discharge and climate variability: 1903 to 1985. Science, 246(4926), 101–103. https://doi.org/10.1126/science.246.4926.101
- Ruault, V., Jouanno, J., Durand, F., Chanut, J., & Benshila, R. (2020). Role of the tide on the structure of the Amazon plume: A numerical modeling approach. *Journal of Geophysical Research*, 125(2), e2019JC015495. https://doi.org/10.1029/2019jc015495
- Salisbury, J., Vandemark, D., Campbell, J., Hunt, C., Wisser, D., Reul, N., & Chapron, B. (2011). Spatial and temporal coherence between Amazon River discharge, salinity, and light absorption by colored organic carbon in western tropical Atlantic surface waters. *Journal of Geophysical Research*, 116(C7), C02028. https://doi.org/10.1029/2011jc006989
- Seidel, M., Dittmar, T., Ward, N. D., Krusche, A. V., Richey, J. E., Yager, P. L., & Medeiros, P. M. (2016). Seasonal and spatial variability of dissolved organic matter composition in the lower Amazon River. *Biogeochemistry*, 131(3), 281–302. https://doi.org/10.1007/s10533-016-0279-4
- Seidel, M., Yager, P. L., Ward, N. D., Carpenter, E. J., Gomes, H. R., Krusche, A. V., et al. (2015). Molecular-level changes of dissolved organic matter along the Amazon River-to-ocean continuum. *Marine Chemistry*, 177, 218–231. https://doi.org/10.1016/j.marchem.2015.06.019
- Seitzinger, S. P., Harrison, J. A., Dumont, E., Beusen, A. H. W., & Bouwman, A. F. (2005). Sources and delivery of carbon, nitrogen, and phosphorus to the coastal zone: An overview of Global Nutrient Export from Watersheds (NEWS) models and their application. *Global Biogeochemical Cycles*, 19(4), GB4S05, https://doi.org/10.1029/2005GB002606
- Sholkovitz, E. R. (1978). The flocculation of dissolved Fe, Mn, Al, Cu, Ni, Co and Cd during estuarine mixing. Earth and Planetary Science Letters, 41(1), 77–86. https://doi.org/10.1016/0012-821x(78)90043-2
- Smith, S. V., & Hollibaugh, J. T. (1993). Coastal metabolism and the oceanic organic-carbon balance. Reviews of Geophysics, 31(1), 75–89. https://doi.org/10.1029/92rg02584
- Smith, W. O., Jr., & Demaster, D. J. (1996). Phytoplankton biomass and productivity in the Amazon River plume: Correlation with seasonal river discharge. Continental Shelf Research, 16(3), 291–319. https://doi.org/10.1016/0278-4343(95)00007-n
- Strub, P. T., Kosro, P. M., Huyer, A., Brink, K. H., Hayward, T., Niiler, P. P., et al. (1991). The nature of the cold filaments in the California
- Current system. *Journal of Geophysical Research*, 96(C8), 14743–14768. https://doi.org/10.1029/91JC01024

  Subramaniam, A., Yager, P. L., Carpenter, E. J., Mahaffey, C., Björkman, K., Cooley, S., et al. (2008). Amazon River enhances diazotrophy and carbon sequestration in the tropical North Atlantic Ocean. *Proceedings of the National Academy of Sciences of the United States of America*, 105(30), 10460–10465. https://doi.org/10.1073/pnas.0710279105
- Twardowski, M. S., & Donaghay, P. L. (2001). Separating in situ and terrigenous sources of absorption by dissolved materials in coastal waters. Journal of Geophysical Research, 106(C2), 2545–2560. https://doi.org/10.1029/1999jc000039
- Varona, H. L., Veleda, D., Silva, M., Cintra, M., & Araujo, M. (2019). Amazon River plume influence on western tropical Atlantic dynamic variability. *Dynamics of Atmospheres and Oceans*, 85, 1–15. https://doi.org/10.1016/j.dynatmoce.2018.10.002
- Ward, N. D., Keil, R. G., Medeiros, P. M., Brito, D. C., Cunha, A. C., Dittmar, T., et al. (2013). Degradation of terrestrially derived macro-molecules in the Amazon River. *Nature Geoscience*, 6(7), 530–533. https://doi.org/10.1038/ngeo1817
- Westberry, T., Behrenfeld, M. J., Siegel, D. A., & Boss, E. (2008). Carbon-based primary productivity modeling with vertically resolved photoacclimation. *Global Biogeochemical Cycles*, 22(2), GB2024. https://doi.org/10.1029/2007GB003078
- Williams, P. M., & Druffel, E. R. M. (1987). Radiocarbon in dissolved organic matter in the central North Pacific Ocean. *Nature*, 330(6145), 246–248. https://doi.org/10.1038/330246a0
- Yamashita, Y., & Tanoue, E. (2004). In situ production of chromophoric dissolved organic matter in coastal environments. *Geophysical Research Letters*, 31(14), GB4S05. https://doi.org/10.1029/2004gl019734

MARTINEAC ET AL. 17 of 17